

## Edge Effects in Vortex-Based Nanocontact Oscillators

C. E. Zaspel

*Department of Environmental Sciences, University of Montana-Western,*

*Dillon, Montana 59725, USA*

G. M. Wysin

*Department of Physics, Kansas State University,*

*Manhattan, KS 66506, USA*

The Oersted field about a nanocontact on a thin film can nucleate vortex formation in the film, and spin torque will drive the vortex in large-amplitude gyrotropic motion about the nanocontact. In a system where the nanocontact is a center of symmetry, the Oersted field provides the restoring force toward the nanocontact center and spin torque balances the dissipation force from damping to give a linear dependence of the gyrotropic frequency on nanocontact current. For the lower symmetry case when the nanocontact is placed close to the edge of a film there is a significant magnetostatic force repelling the vortex from the edge as well as a deformation of the vortex structure. Both effects combine to produce an anisotropic restoring force, which in turn result in the existence of a lower critical current for gyrotropic motion and a nonlinear dependence of the gyrotropic frequency on the nanocontact current.

PACS numbers: 75.75.Jn, 75.70.Kw, 75.40.Gb

## Introduction

The magnetic vortex is a domain structure that has attracted much theoretical and experimental interest during the past twenty years owing to the fact that it can be the ground state [1,2] in a ferromagnetic nanodisk. This is the result of competition between exchange and the dipole-dipole interaction giving in-plane curling of the magnetization which minimizes magnetostatic poles at the disk edge. There is, however, a small-radius (5-10 nm for permalloy) out-of-plane vortex core at the vortex center which eliminates the exchange singularity. The small size of submicron disks make them excellent candidates for devices operating in the microwave region of the spectrum. Indeed, the lowest frequency dynamic excitation corresponds to a high amplitude sub-GHz gyrotropic precession [3-5] of the vortex core about the disk center where the gyro-force is opposed by a magnetostatic force directed toward the disk center. For this type of motion in the disk the precession frequency is proportional [6, 7] to  $L/R_D$  where  $L$  and  $R_D$  are the disk thickness and radius, respectively. More recently it has been shown that steady state gyrotropic motion can be established [8, 9] in a nanopillar through a spin-polarized current, where oscillation sets in above a critical current [10] and the power added to the system by spin torque balances the energy lost to dissipation.

One disadvantage of the nanopillar oscillator is the lack of a simple external frequency control since the frequency depends on the disk dimensions. This can be overcome by use of a nanocontact oscillator consisting of a nanocontact on a fixed and free layer where steady state gyrotropic motion [11] was first observed, but not recognized as such. Later experimental and theoretical work showed that the Oersted field from the nanocontact current results in formation of a vortex [12] and it also provides the restoring force necessary to give gyrotropic motion in an elliptical orbit about the nanocontact. Experimentally [11] it is noticed that after the vortex is

formed a current decrease will result in a linear frequency decrease until a lower current is reached where gyrotropic motion is no longer sustained. However, theoretical work [12] does not indicate the existence of a lower critical current in contrast to the spin torque driven nanopillar. Additionally, the fact that the frequency is proportional to the nanocontact current provides an effective external control of the oscillator frequency.

Since vortex formation and gyrotropic motion driven by spin torque are possible in both nanopillars and nanocontacts, it is instructive to compare these two systems and notice similarities and differences. Both require a gyroforce and a restoring force where the gyroforce is independent of the system parameters and only dependent on the vortex structure. However, the form of the restoring force has a different functional form depending on the confining potential: For the case of the circular disk the magnetostatic energy minimum is located at the disk center with the usual harmonic oscillator displacement dependence. The vortex formed at a nanocontact is confined by the Oersted field with the minimum energy at the nanocontact center, but the dependence on vortex displacement is linear. This difference in the confining potential leads to the differences in the calculated orbit parameters in these systems, namely the existence of a critical current with a current-dependent orbit radius [10] in the nanopillar, and in the nanocontact an orbit radius independent of the current without a critical current [12]. The fact that the orbit radius is independent of nanocontact current implies that the vortex-based nanocontact oscillator has infinite agility [13], or an abrupt current change can result in an abrupt frequency change. For all previous theoretical models the magnetostatic energy has not been considered in nanocontact systems on ferromagnetic thin films owing to the assumption that the vortex is not confined by edges.

In this article the effect of magnetostatic energy from a film edge on nanocontact vortex dynamics is investigated theoretically. The source of magnetostatic energy is an edge of a semi-infinite thin film with the nanocontact placed near the film edge, and the effect of the edge on the current-dependent frequency is investigated. It is also shown that an edge will result in the existence of a lower critical current below which gyrotropic motion about the nanocontact will no longer be sustained. In previous work for the case of the disk, the magnetostatic energy is minimized through elimination of magnetostatic surface charge at the disk edge, which is accomplished by requiring zero magnetization normal to the edge. For motion of a vortex off the disk center the image charge ansatz [6] is used to ensure zero edge charge at the expense of volume magnetostatic charge resulting in a quadratic restoring potential,  $W_{MS} \propto X^2 + Y^2$  where  $X$  and  $Y$  are the coordinates representing vortex core displacement from the disk center. A similar method is used here for the nanocontact on a film with the nanocontact close (1000-3000 nm) to the film edge. Complex variable methods [14] are used to obtain a magnetization ansatz having zero edge charge, which is used to numerically calculate both the magnetostatic and Oersted energies for the vortex as a function of its position in the film. Next a Thiele equation containing damping and spin-polarized current forces is solved to obtain vortex core gyrotropic orbits and frequencies about the nanocontact in the free-layer. It is noticed that edge magnetostatic effects will repel the vortex from the edge, which combines with the Oersted field tending to attract the vortex to the nanocontact. The net effects on vortex dynamics are shown to be an acceleration of the vortex core and distortion of the orbit shape corresponding to an increase in eccentricity of the orbit. These effects lower the orbital frequency and provide the mechanism for the existence of a lower critical current where the vortex will become fixed at an equilibrium position not necessarily at the nanocontact center.

## Dynamics Equation

It is convenient to use a collective variable approach to describe the motion of a vortex driven by spin torque, where  $\vec{X}_v = (X(t), Y(t))$  is the time-dependent location of the vortex core in the upper half  $xy$  plane of the free layer. The normalized magnetization in the free layer is given by  $\vec{M} = M_s (m_x, m_y, m_z)$  where  $M_s$  is the saturation magnetization. Assuming that the time dependence of the magnetization is a result of vortex motion, the normalized components can be expressed as  $m_x = m_x(x - X(t), y - Y(t), z)$  with a similar expression for the  $y$ -component. Also it is assumed that the film thickness is very small compared to other dimensions so motion will be confined to the  $xy$  plane and the magnetization is uniform in the  $z$ -direction. Then the Landau-Lifshitz-Gilbert equation with spin torque can be expressed as a Thiele [15, 16] equation

$$\vec{G} \times \dot{\vec{X}}_v + \frac{\partial W(\vec{X}_v)}{\partial \vec{X}_v} = -D\dot{\vec{X}}_v + \vec{F}_{ST}, \quad (1)$$

where  $\vec{G} = 2\pi\mu_0 M_s L \hat{z} / \gamma$  is the gyrovector containing the free layer thickness,  $L$  and the gyromagnetic ratio,  $\gamma$ . The energy  $W$  contains conservative contributions such as the magnetostatic energy and the Oersted energy of the vortex in the magnetic field from the nanocontact current. Nonconservative forces are on the right hand side, which include the damping and spin torque forces.

The key point of this article is the calculation of the Oersted and magnetostatic energies by selection of an appropriate magnetization ansatz to take into account the edge effects. Recently Metlov [14] has developed a technique to obtain a magnetization structure that will minimize various energies sorted by order of decreasing importance. This technique begins with the normalized magnetization expressed as a stereographic projection,

$$m_x + im_y = \frac{2w(z, \bar{z})}{1 + |w(z, \bar{z})|^2}, \quad m_z = \frac{1 - |w(z, \bar{z})|^2}{1 + |w(z, \bar{z})|^2} \quad (2)$$

where  $z = x + iy$  and the bar indicates complex conjugation and the complex function,  $w(z, \bar{z})$  is chosen to minimize the energy. In nanoscale systems exchange is typically the most important term and isotropic exchange is minimized by the choice of any analytic function. In particular, here we are interested in vortices having a meron [17] structure further restricting the function to the form,  $w(z, \bar{z}) = f(z) / \sqrt{f(z)\bar{f}(\bar{z})}$ , where  $f(z)$  is an arbitrary analytic function. Notice that  $m_z = 0$  everywhere, so the meron ansatz will be a very good representation of the actual vortex outside of the vortex core, which is very small (the order of 5-10 nm for permalloy) compared to all other length parameters. Indeed, the expression for the gyrovectector in Eq. (1) is obtained through the assumption that the vortex core is a delta-function. Since the exchange energy is minimized by this arbitrary function, any variation of the exchange energy resulting from a small change in the vortex core position is negligible compared to other contributions considered in the following. Next in order of importance is the magnetostatic energy, which can originate from both edge and volume magnetostatic charge. It has been shown [6] that elimination of the edge magnetostatic charge at the expense of volume magnetostatic charge agrees very well with micromagnetic calculations applied to the circular disk. In principle, magnetostatic edge charge can be zeroed [14] for a general shape nanoparticle through a series of conformal mappings to the desired final shape. However, for the particular case of the single vortex in the semi-infinite plane, the function resulting in zero edge charge on the  $x$ -axis ( $y = 0$ ) has the simple form

$$f(z, \bar{z}) = (Z - z)(\bar{Z} - \bar{z}), \quad (3)$$

where  $Z = X + iY$  is the complex position of the vortex core. This ansatz results in a deformed vortex with a corresponding increase in volume magnetostatic charge ( $\vec{\nabla} \cdot \vec{m}$ ) so it is necessary to

calculate this contribution to the magnetostatic energy as well as the Oersted energy from the nanocontact current using this magnetization ansatz.

All terms in the Thiele equation are obtained using Eqs. (2, 3) with the form of the vortex and the coordinate system illustrated in Fig. 1, showing the vortex structure with its center on the  $y$ -axis and zero normal magnetization on the  $x$ -axis. In Fig. 1 the edge of the film is defined by the  $x$ -axis and later when the nanocontact is included, it will be on the  $y$ -axis at coordinate  $Y_0$ . Notice here the definite distortion of the vortex structure due to elimination of the magnetostatic edge charge. The energy and additional coefficients in Eq. (1) are evaluated by integration over the upper half plane, and since Eq. (3) does not contain the core structure. Therefore, all integrals used to calculate terms of Eq. (1) are evaluated with the small vortex core region neglected, which simplifies the numerical integration with a negligible effect on the integral value for the length parameters considered here.

First the parameters in the nonconservative forces are determined. The simplest form for the Gilbert damping coefficient [18] is

$$D = \alpha \frac{\mu_0 M_s}{\gamma} L \iint (\bar{\nabla} \varphi)^2 dx dy, \quad (4)$$

where  $\alpha \approx 0.01$ ,  $\varphi(x, y) = \tan^{-1}(m_y/m_x)$  is the azimuthal angle of the magnetization from Eqs. (2, 3), and the integral is over the rectangular region,  $-R \leq x \leq R$  and  $0 \leq y \leq R$  with fixed boundary conditions on the  $x$ -axis and free boundary conditions at  $y = R$  and  $x = \pm R$ . For the single vortex in a circular disk this term has a  $\ln(R_D/l_0)$  dependence with the  $l_0$  cut-off which is typically the vortex core radius. Using the magnetization ansatz the integral in Eq. (4) cannot be done analytically, but numerical evaluation of the integral in Eq. (4) indicates that it can be approximated by the function  $28 + 3.08 \ln(R/Y)$ , agreeing with the numerical integration to

within a few percent for parameters considered here. This results in a simple  $Y$ -dependent expression for  $D$  to be used in the solution of the Thiele equation.

To obtain the force on the vortex from spin torque, a detailed picture of the electron transport is required. In earlier analytic work [12] it was assumed that the nanocontact current was perpendicular to the fixed and free layers. However, more recent [19] numerical current density calculations have shown that the electron flow is mainly perpendicular to the nanocontact plane (CPP) in the nanocontact itself, and mostly in-plane (CIP) in the layers. To proceed with analytical calculations it is necessary to assume an idealized model representing the current, which is illustrated in Fig. 2 where the arrows represent a simplified electron flow. Within the nanocontact probe, the current,  $I_{CPP}$ , is perpendicular to the plane in a cylinder of radius,  $r_0$ . Where the nanocontact probe connects to the film it is assumed that the electron flow goes from CPP to CIP in the fixed and free layers.

The presence of the edge lowers the symmetry of this system, which will also have an effect on the currents as well as the Oersted field about the nanocontact and the magnitude of the spin torque force. Recent simulations [20] have shown that both CIP and CPP distributions depend on the structure of the nanocontact layers as well as the nanocontact-edge separation,  $Y_0$ . For the CPP case it was found that this component of the current is confined mainly to the inside of the nanocontact and it decreases very rapidly outside of the nanocontact edge. On the other hand, the CIP is more strongly modified from cylindrical symmetry owing to the edge, and it was shown [20] that the current density has the form,  $j = j_{cyl} + \Delta j$  where  $j_{cyl}$  is the symmetric current density,  $\Delta j$  is the maximum deviation from cylindrical symmetry given by  $\Delta j \propto r/Y_0$ , valid for the case when the vortex center is between the nanocontact position and the edge, and  $r$  is the vortex center distance from the nanocontact center. Later it will be shown that the small

deviation condition will be well-satisfied so it will be appropriate to use the cylindrical approximation.

It has recently been shown [21] that the dominant contribution to spin torque is the in-plane current. For this case, the spin-torque term [22] in the Landau-Lifshitz equation is

$\Gamma_{ST} = (\vec{u} \cdot \vec{\nabla}) \vec{m}$ , where  $\vec{u}$  is the in-plane spin current density. When this is converted to the spin torque force in the Thiele equation one has the following integral to evaluate

$$\vec{F}_{ST} = -\frac{\mu_0 M_s}{\gamma} \int \sin \theta (\vec{\nabla} \varphi \times \vec{\nabla} \theta) \times \vec{u} d^3 r, \quad (5)$$

where the integral is over the system volume. For the case of the vortex structure of Fig. 1 this can be integrated by assuming that the vortex core is a  $\delta$ -function core and changes in  $\vec{u}$  across the core can be neglected. This gives the simple expression for the spin torque force

$$\vec{F}_{ST} = \vec{G} \times \vec{u}(\vec{R}_v), \quad (6)$$

depending on the separation between the nanocontact center and the vortex core,

$R_v = \sqrt{X^2 + (Y - Y_0)^2}$ . When the cylindrical symmetry approximation is valid the spin current density in the free layer is

$$\vec{u} = P \frac{\hbar \gamma}{2e\mu_0 M_s} j(r) \hat{r}, \quad (7)$$

in the radial ( $\hat{r}$ ) direction relative to the nanocontact center, where  $r = \sqrt{x^2 + (y - Y_0)^2}$ ,  $e$  is the electron charge,  $\gamma$  is the gyromagnetic constant of the free layer and  $P$  is a polarization efficiency. Referring to Fig. 2 the current density is assumed to have the radial form,

$$\vec{j}(r) = \frac{I_{CIP} \hat{r}}{2\pi r_0 L} \begin{cases} r/r_0 & r < r_0 \\ r_0/r & r > r_0 \end{cases}. \quad (8)$$

This current density gives the spin torque force

$$\vec{F}_{ST} = G\sigma \frac{I_{CIP}}{\sqrt{X^2 + (Y - Y_0)^2}} \hat{\chi} \quad (9)$$

in the azimuthal direction ( $\hat{\chi}$ ) relative to the nanocontact center, where  $\sigma = \hbar\gamma/4\pi e\mu_0 M_s L$ .

Notice that the force in Eq. (9) only depends on the coordinates of the vortex center, so if the vortex center remains far from the film edge, the radial symmetry approximation will be valid.

According to the simulations in Ref. [20] the deviation from cylindrical symmetry will approach about 10% closer to the edge. Later when vortex orbits are calculated it will be noticed that there is a current range where the vortex core remains far from the edge so the cylindrical symmetry of the current density will remain a good approximation. In the following the coordinates  $(x, y)$  and  $(X, Y)$  are defined according to the axes of Fig. 1.

### Energy Calculation

Next the conservative contributions to the Oersted and magnetostatic energies are calculated, where anisotropy from the effect of the edge on the vortex structure is important. The Oersted energy is obtained for the nanocontact at  $Y_0$  on the  $y$ -axis as in Fig. 1, which involves the calculation of the Zeeman energy for the vortex in the Oersted field. For the simplified nanocontact structure of Fig. 2 it is assumed that the Oersted field in the free layer is obtained from the Biot-Savart law applied to a semi-infinite straight wire,  $B = \mu_0 I_{CPP}/4\pi r$  outside of the nanocontact and  $B = \mu_0 I_{CPP} r/r_0^2$  inside the nanocontact, where  $r$  is the distance from the nanocontact center. For the simplest case when asymmetric edge effects are not taken into account [12] this energy is a linear function ( $W_{Oe} = \kappa \sqrt{X^2 + (Y - Y_0)^2}$ ) of the vortex core-nanocontact separation and it has azimuthal symmetry about the nanocontact. Even for this

simplest case the value of  $\kappa$  must be obtained by numerical integration. For the geometry of Fig. 1 (the electron flow is in the  $-\hat{z}$  direction) the Oersted energy is

$$W_{Oe} = \frac{\mu_0 M_s I_{CPP} L}{4\pi} \int \frac{m_x (Y_0 - y) + m_y x}{x^2 + (y - Y_0)^2} dx dy, \quad (10)$$

where the integration is over the free layer in the upper half plane. Evaluation of these types of integrals for a vortex magnetization distribution is typically done neglecting the small out-of-plane core. As long as the core is much smaller than the vortex size ( $Y_0$  or  $R$ ) the core contribution will be negligible. Numerical integration of Eq. (10) over the region  $-R \leq x \leq R$  and  $0 \leq y \leq R$  also exhibits an approximate linear dependence relative to the vortex core-nanocontact displacement,  $R_V = \sqrt{X^2 + (Y - Y_0)^2}$ , with a quadratic correction. To better illustrate the difference between the vortex positions,  $Y < Y_0$  and  $Y > Y_0$ , the Oersted energy density,

$u_{Oe} = W_{Oe}/V$  is calculated, where  $V = 2LR^2$  is the volume of the free layer. It can be seen that the Oersted energy density is proportional to  $\mu_0 M_s^2 R_B / R^2$ , where  $\mu_0 M_s^2$  has units of energy density, and the result is linearly proportional to  $I_{CPP} / M_s \equiv R_B$  which is the length scale over which the Oersted field is significant, measured from the nanocontact center. For the vortex center confined to the  $y$ -axis, Fig. 3a clearly illustrates the approximate linear dependence of  $u_{Oe}$  for  $Y > Y_0$  and the more pronounced quadratic dependence for  $Y < Y_0$ . The integrations over  $x$  and  $y$  out to the size parameter  $R$  cause  $u_{Oe}$  to scale with  $1/R$ . As a result, the Oersted energy density is proportional to  $I_{CPP} / M_s R$ . To show results valid for any current value, the Oersted energy density divided by Oersted length  $R_B$  and multiplied by  $R$  is shown in Fig. 3b. These two figures indicate that  $u_{Oe}$  is proportional to  $R_B / R$ . However, as noticed in Fig. 3a,b there is asymmetry in the azimuthal direction relative to the nanocontact center. Numerical

evaluation of the integral in Eq. (10) with the vortex core off of the  $y$ -axis indicates that a very good approximation for the Oersted energy is

$$W_{Oe} = \frac{\mu_0 M_s I_{CPP} L}{4\pi} \left[ (\beta + \Delta\beta \sin \chi_V) R_V - \gamma (1 - \sin \chi_V) R_V^2 \right], \quad (11)$$

where  $\chi_V = \sin^{-1}[(Y - Y_0)/R_V]$  is the azimuthal coordinate of the vortex core relative to the nanocontact. Parameter values obtained numerically are shown in Fig. 4 where it is noticed that the linear parameters are weak functions of  $Y_0$ .

The magnetostatic energy is obtained from the magnetostatic field expressed as a partial derivative of the magnetostatic potential,

$$\Phi = \frac{-M_s}{4\pi} \int \frac{\vec{\nabla} \cdot \vec{m} \, dx' dy' dz'}{\sqrt{(x-x')^2 + (y-y')^2 + (z-z')^2}}. \quad (12)$$

First the integration over  $z'$  can be done assuming that  $z \cong 0$  for the free layer, and next the partial derivative gives the magnetostatic field in the  $x$ -direction,

$$H_x = -\partial_x \Phi = -\frac{M_s L}{4\pi} \int \frac{(x-x') \vec{\nabla} \cdot \vec{m}(x', y') dx' dy'}{(\bar{r} - \bar{r}')^2 \sqrt{(\bar{r} - \bar{r}')^2 + L^2/4}}, \quad (13)$$

where  $(\bar{r} - \bar{r}')^2 = (x-x')^2 + (y-y')^2$ , with a similar expression for  $H_y = -\partial_y \Phi$ . Using this magnetostatic field and the normalized magnetization  $\vec{m}$ , the integral giving the magnetostatic energy becomes another two-dimensional integral, and in general the magnetostatic energy is

$$W_{MS} = \frac{-\mu_0 M_s L}{2} \int (m_x H_x + m_y H_y) d^2 \vec{r}, \quad (14)$$

containing an additional factor of  $L$  from the integration over  $z$ . Notice that Eq. (14) leads to a four-dimensional integral when combined with Eq. (13) and it is seen that  $W_{MS}$  should scale with  $M_s^2 L^2$ . For the much simpler case of a vortex in a circular disk, three of these integrations can be

done analytically in terms of elliptic integrals with a single numerical integration remaining. Owing to this simplification in the disk structure it is possible to obtain the magnetostatic energy in the harmonic oscillator [6] form,  $W_{MS} = k(X^2 + Y^2)/2$  where  $k = 0.15 L^2/R_D$  for a disk of radius,  $R_D$  with the vortex position measured relative to the disk center. However, for the lower symmetry magnetization of Eqs. (2, 3), the four-dimensional integral must be done numerically and the results do not have a simple dependence on the system geometry. Integration at fixed system size  $R = 10^5$  nm indicates that the magnetostatic energy is indeed proportional to  $L^2$  and integration for a fixed  $L = 2$  nm for various values of  $R$  indicates that the magnetostatic energy is proportional to the system size,  $R$ . The magnetostatic energy density,  $u_{MS} = W_{MS}/V$ , can also be presented as a curve independent of the system size for the free layer thickness,  $L = 2$  nm as shown in Fig. 5. Moreover, it is remarked that this graph is well-approximated by the equation having a simple  $Y/R$  dependence, and since the energy density is proportional to  $1/R$ , the magnetostatic energy is approximately,

$$W_{MS} = \mu_0 M_s^2 L^2 R \left( -0.339 + \frac{1.04}{(1 + Y/R)^2} \right) \quad (15)$$

as a function of the vortex coordinate,  $Y$ . In the following  $L = 2$  nm and  $R = 10^5$  nm, so this large value of  $R$  will ensure that the vortex center will be far from the free boundary and  $W_{MS}$  will also be independent of  $X$ . Notice that the fixed edge at  $y = 0$  tends to repel the vortex owing to the increased volume magnetostatic charge as the vortex approaches the edge.

Finally, the Oersted and magnetostatic energies are combined to give  $W(\vec{X}_v)$  and the conservative forces in Eq. (1). Notice that the Oersted force will tend to attract the vortex center to the nanocontact and the magnetostatic force will repel the vortex from the edge, so the vortex

equilibrium position in the absence of spin torque will tend to be on the  $y$ -axis with  $Y > Y_0$ . For a large enough current it is expected that the vortex will remain confined to an orbit about the nanocontact when the energy added by spin torque compensates energy loss from damping. However, in contrast to the theoretical results applied to the symmetric nanocontact film, there will be a critical current below which the vortex will remain fixed at the equilibrium position outside of the nanocontact. This is considered in the next section regarding vortex dynamics forced by spin torque.

### **Solution of the Thiele Equation**

Next Eq. (1) is solved numerically using the approximate functional forms for damping and energy to obtain critical currents for vortex orbital motion as well as the current-dependent frequencies and orbits. Since  $\sigma \approx 1/r_0^2$  it is noticed that the spin torque term is independent of the nanocontact radius, but there is a small effect from  $r_0$  resulting from the integration to obtain the Oersted energy. In the following the parameters applicable to permalloy are used,  $\mu_0 M_s = 1$  T,  $2M_s\gamma = 30$  GHz,  $P = 0.2$  and  $\alpha = 0.01$  for a free layer thickness,  $L = 2$  nm. Referring to Fig. 2, the nanocontact  $I_{CPP}$  splits into in-plane components in both the fixed and free layers and the actual magnitudes of these components depend on the nanocontact structure, which is not possible to calculate analytically. However, when  $I_{CIP}$  represents only the current in the free layer it is obvious that  $I_{CPP} > I_{CIP}$  with the actual difference dependent on the nanocontact as well as the structure of the various layers. For the following calculations it is assumed that  $I_{CIP} = I_{CPP}/2$ , corresponding to equal free and fixed layer thickness.

Recall that for the disk-shaped nanopillar there is a critical current below which the vortex core will remain at the disk center. A similar critical current,  $I_c$  is shown to exist by

numerical solution of Eq. (1) using Mathematica. Initially the vortex center is on the  $y$ -axis about 20 nm outside of the nanocontact and after a time of 1000 ns the vortex center either goes to a fixed point outside of the nanocontact or defines a stable elliptical orbit about the nanocontact. First, a static solution with  $\dot{X} = 0$  and  $\dot{Y} = 0$  at low current values is obtained, where the  $x$  and  $y$ -components of the conservative and spin torque forces balance. These results are presented in Fig. 6 for the nanocontact at  $Y_0 = 300$  nm, with the solid curve representing the  $y$  component of the vortex center ( $Y$ ) and the dashed curve representing the  $x$  component of the vortex center ( $X$ ) as functions of  $I_{CPP}$ . The  $x$  components of the Oersted and spin torque force are both linear in current so the  $x$  component of the static position is only weakly dependent on current as seen on the right hand axis of Fig. 6. However, the  $y$  component of these forces contains an additional magnetostatic term so owing to the lower symmetry. The static position of the vortex exhibits a much stronger dependence on the nanocontact current owing to the fact that the Oersted force and the magnetostatic force are in opposite directions for  $Y > Y_0$ .

Above the critical current the vortex core will move in an elliptical orbit about the nanocontact and numerical solution gives the orbits and frequencies. These data are obtained for nanocontact positions,  $Y_0$  at 300, 3000, and 10,000 nm and the frequency versus current data are illustrated in Fig. 7. It is remarked that these frequencies are lower than the frequencies observed [11, 12] at similar current ranges. This is due to the decreased restoring force because of the opposite directions of the Oersted and magnetostatic forces as noted previously. Notice that for each curve the frequency drops to zero as the current decreases to a minimum where the vortex becomes fixed, defining the critical current,  $I_c$  as a function of  $Y_0$  shown in the inset graph of Fig. 7. It is also remarked there is a definite frequency nonlinearity immediately above  $I_c$  and

the slope in the linear region at higher current values exhibits a slight dependence on current with a slope of 1.10 MHz/mA for  $Y_0 = 300$  nm and a slope of 1.62 MHz/mA for  $Y_0 = 10,000$  nm.

The origin of this nonlinearity can be better understood by referring to Fig. 8, showing a typical orbit for  $Y_0 = 3000$  nm with  $I_{CPP} = 8$  mA, a value slightly above the critical current.

Notice that the closest approach of the vortex center to the nanocontact is at a value of  $Y_{\min} < Y_0$  and the furthest distance satisfies  $Y_{\max} > Y_0$ , also because of damping the orbit is tilted relative to the  $y$  axis. Next let us consider the actual distance of the vortex center from the nanocontact,  $R_V$ , where the maximum and minimum values versus current are plotted in Fig. 9 for  $Y_0 = 300$  nm.

The solid curves representing these values indicate that the vortex center approximately follows an elliptic orbit with the nanocontact at one focal point with the eccentricity increasing as the current approaches  $I_c$ . Using the Kepler's second law analogy it is expected that the vortex velocity will decrease as  $R_V$  decreases and the dashed curves show that this is indeed the case.

Owing to the high eccentricity of the orbit and the corresponding decrease of vortex velocity there is a nonlinearity in the frequency versus current graph as seen in Fig. 7. Finally, Fig. 9 indicates that there is a slight eccentricity increase for higher currents; this is probably the result of increased edge effects as  $R_V$  increases with current. Revisiting the cylindrical symmetry current approximation, Fig. 9 shows that the vortex center will always be far from the edge, or  $(Y - Y_0)/Y_0 \ll 1$  so there will always be a current range above  $I_c$  where  $\Delta j$  is small. For the smallest value of  $Y_0 = 300$  nm this approximation is no longer valid as the current approaches  $I_c$ ; however, in the range  $300 < Y_0 < 10,000$  nm the cylindrical symmetry approximation is valid for all current values.

## Conclusion

In summary, the effect of an edge on the dynamics of a vortex formed at a nanocontact on a thin film is investigated with magnetostatic effects taken into account. The existence of the edge and a corresponding elimination of edge magnetostatic charge results in an anisotropy of the vortex structure relative to the nanocontact. This effect gives a significant anisotropy to the Oersted energy, which is the source of the restoring force on the vortex in a typical nanocontact system. Since the edge has an effect on the vortex structure, there is also a nonzero volume magnetostatic charge, which results in a repelling magnetostatic force on the vortex from the edge. The force from spin torque in the azimuthal direction relative to the nanocontact drives the vortex core in its orbit. As is also the case for the nanopillar, there is a critical current above which the vortex core will remain in a stable orbit about the nanopillar, but below the critical current the spin torque, Oersted, and magnetostatic forces combine to move the vortex to an equilibrium position off of the nanocontact center. Above the critical current the orbit has an approximate elliptical shape of high eccentricity immediately above the critical current and an almost circular shape at higher current values.

In general, it is remarked that the presence of an edge close to the nanocontact will significantly modify the orbit shape from an approximate circle to a high eccentricity ellipse for nanocontact current values approaching the critical current. Also if the edge is at a sufficient distance from the nanocontact, resulting in a low enough critical current, then a slowing of the vortex core in its orbit will result in a nonlinear dependence of orbital frequency on nanocontact current.

## References

- [1] J. Raabe, R. Pulwey, S. Sattler, T. Schweinbock, J. Zweck, and D. Weiss, *J. Appl. Phys.* **88**, 4437 (2000).
- [2] K. Y. Guslienko, V. Novosad, Y. Otani, and K. Fukamichi, *Appl. Phys. Lett.* **78**, 3848 (2001).
- [3] B. E. Argyle, E. Terrenzio, and J. C. Slonczewski, *Phys. Rev. Lett.* **53**, 190 (1984).
- [4] J. P. Park, P. Eames, D. M. Engebretson, J. Berezovsky, and P. A. Crowell, *Phys. Rev. B* **67**, 167201 (2005).
- [5] S. -B. Choe, Y. Acremann, A. Scholl, A. Bauer, A. Doran, J. Stöhr, and H. A. Padmore, *Science* **304**, 420 (2004).
- [6] K. Y. Guslienko, B. A. Ivanov, V. Novosad, Y. Otani, H. Shima, and K. Fukamichi, *J. Appl. Phys.* **91**, 8037 (2002).
- [7] B. A. Ivanov and C. E. Zaspel, *Appl. Phys. Lett.* **95**, 7444 (2004).
- [8] S. Kasai, Y. Nakatani, K. Kobayashi, H. Kohno, and T. Ono, *Phys. Rev. Lett.* **97**, 107204 (2006).
- [9] V. S. Pribiag, I. N. Krivorotov, G. D. Fuchs, P. M. Braganca, O. Ozatay, J. C. Sankey, D. C. Ralph, and R. A. Buhrman, *Nature Phys.* **3**, 498 (2007).
- [10] A. V. Khvalkovskiy, J. Grollier, A. Dussaux, K. A. Zvezdin, and V. Cros, *Phys. Rev. B* **80**, 140401(R) (2009).
- [11] M. R. Pufall, W. H. Rippard, M. L. Schneider, and S. E. Russek, *Phys. Rev. B* **75**, 140404(R) (2007).
- [12] Q. Mistral, M. van Kampen, G. Hrkac, Joo-Von Kim, T. Devolder, P. Crozat, C. Chappert, L. Lagae, and T. Schrefl, *Phys. Rev. Lett.* **100**, 257201 (2008).

- [13] M. Manfrini, T. Devolder, Joo-Von Kim, P. Crozat, N. Zerounian, C. Chappert, W. Van Roy, L. Lagae, G. Hrkac, and T. Schrefl, *Appl. Phys. Lett.* **95**, 192507 (2009).
- [14] K. L. Metlov, *Phys. Rev. Lett.* **105**, 107201 (2010).
- [15] A. A. Thiele, *Phys. Rev. Lett.* **30**, 230 (1973).
- [16] D. L. Huber, *Phys. Rev. B* **26**, 3758 (1982).
- [17] D. L. Gross, *Nucl. Phys.* **B132**, 439 (1978).
- [18] K. Y. Guslienko, *Appl. Phys. Lett.* **89**, 022510 (2006).
- [19] E. Jaromirska, L. Lopez-Diaz, A. Ruotolo, J. Grollier, V. Cros and D. Berkov, *Phys. Rev. B* **83**, 094419 (2011).
- [20] S. Petit-Watelot, R. M. Otxoa and M. Manfrini, *Appl. Phys. Lett.* **100**, 083507 (2012).
- [21] S. Petit-Watelot, Joo-Von Kim, A. Rutolo, R. M. Otxoa, K. Bouzehouane, J. Grollier, A. Vansteenkiste, B. Van de Wiele, V. Cros and T. Devolder, *Nature-Phys.* **8**, 682 (2012).
- [22] S. Kasai, Y. Nakatani, K. Kobayashi, H. Kohno and T. Ono, *Phys. Rev. Lett.* **97**, 107204 (2006).

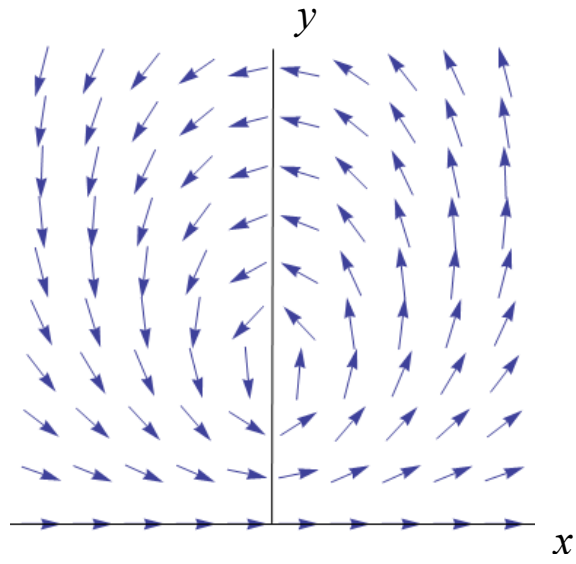


Fig.1. Vortex structure specified by Eqs. (2, 3) with the vortex core on the  $y$ -axis. The  $x$ -axis is the film edge and the nanocontact will be confined to the  $y$ -axis in the following.

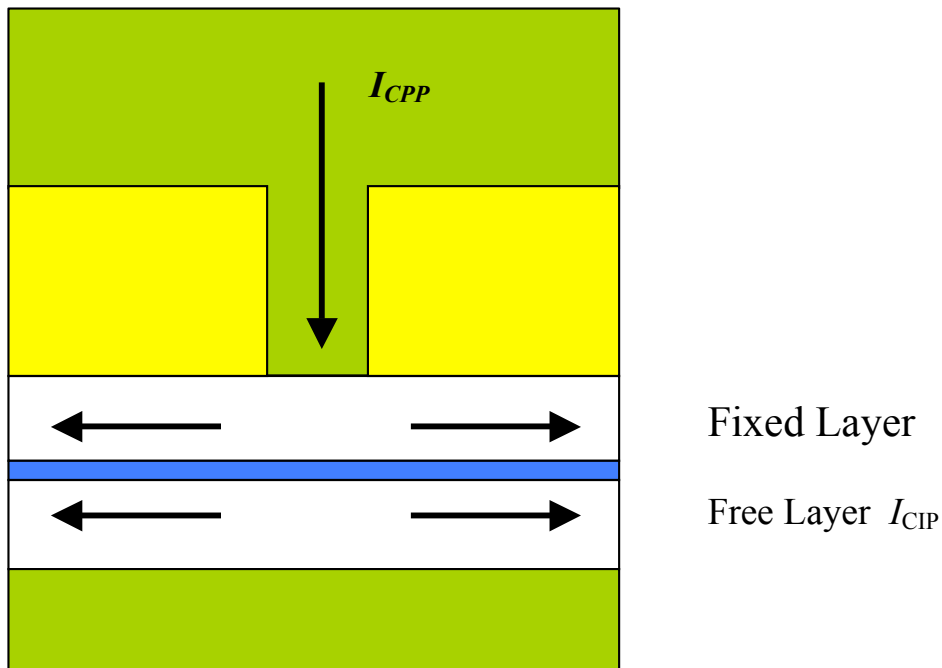
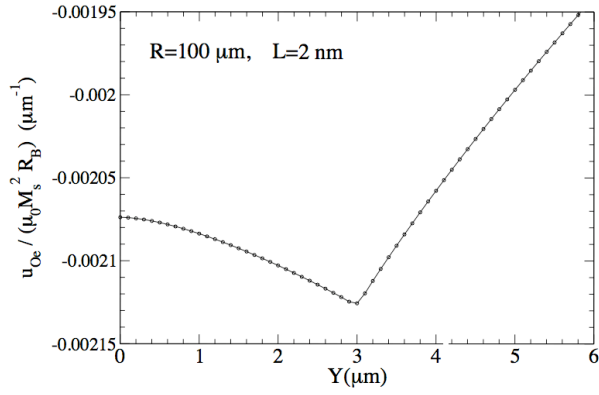
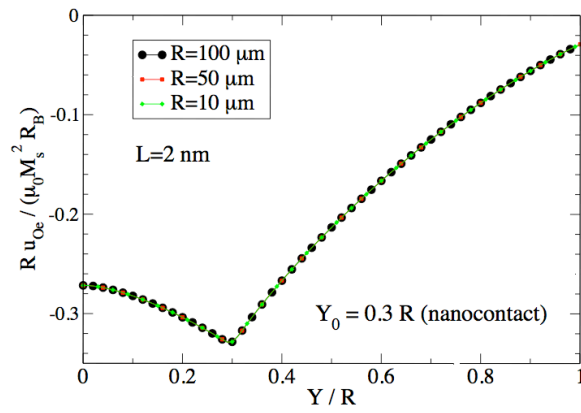


Fig. 2. Simplified nanocontact structure where green indicates a conductor, white indicates a ferromagnetic material such as permalloy and blue indicates a spacer.  $I_{CPP}$  is the current indicated by the arrow above the layers and  $I_{CIP}$  is the free layer current.



a)



b)

Fig. 3. Oersted energy density for a vortex at  $\vec{X}_v = (0, Y)$  near a nanocontact on the  $y$ -axis at  $(0, Y_0)$ . In a) the Oersted energy density divided by Oersted length  $R_B = I/M_s$  is shown for a nanocontact at  $Y_0 = 3.0 \mu\text{m}$ . In b) results on different sized systems scaled by system size  $R$  all fall on the same curve, showing that the Oersted energy density is proportional to  $R_B/R$ .

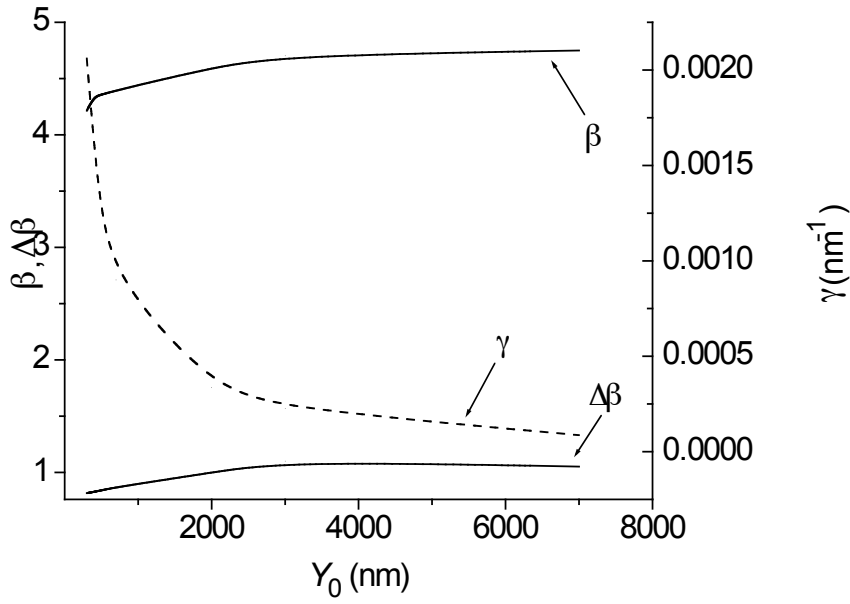


Fig. 4. Parameter values in Eq. (11) versus  $Y_0$ . Solid curves represent  $\beta$  and  $\Delta\beta$ , and the dashed curve represents  $\gamma$ . The  $\beta$  parameters are dimensionless.

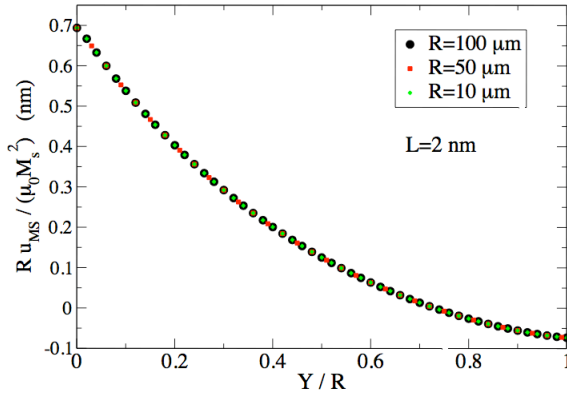


Fig. 5. Magnetostatic energy density  $u_{MS} = W_{MS}/V$  for a vortex at position  $\vec{X}_v = (0, Y)$ , in systems of the same thickness  $L$  but different lateral size parameters  $R$ . The independence of the results on  $R$  shows that  $u_{MS} \propto 1/R$  and leads to  $W_{MS}$  having the form given in Eq. (15).

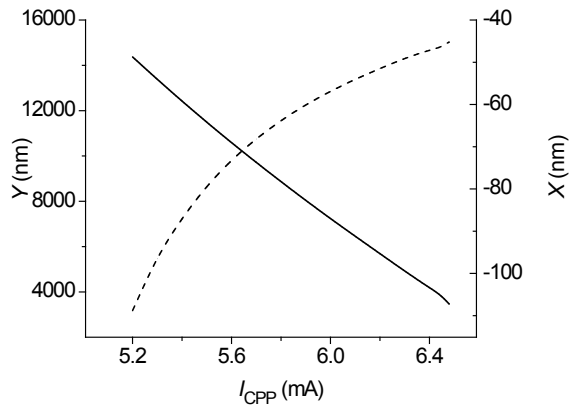


Fig. 6. Static vortex core position versus nanocontact current for  $I < I_c$  with the nanocontact at  $Y_0 = 3000$  nm. Solid curve,  $Y$ ; dashed curve,  $X$ .

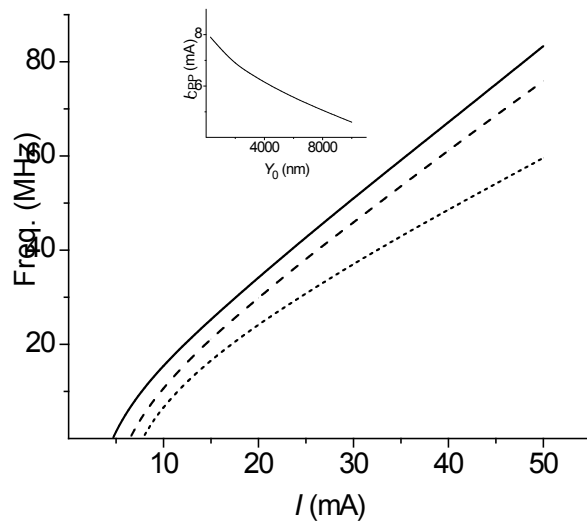


Fig. 7. Gyrotropic frequency versus nanocontact current for three nanocontact positions. Solid  $Y_0 = 10,000$  nm, dashed  $Y_0 = 3000$  nm, and short dashed  $Y_0 = 300$  nm. Inset shows the critical current versus  $Y_0$ .

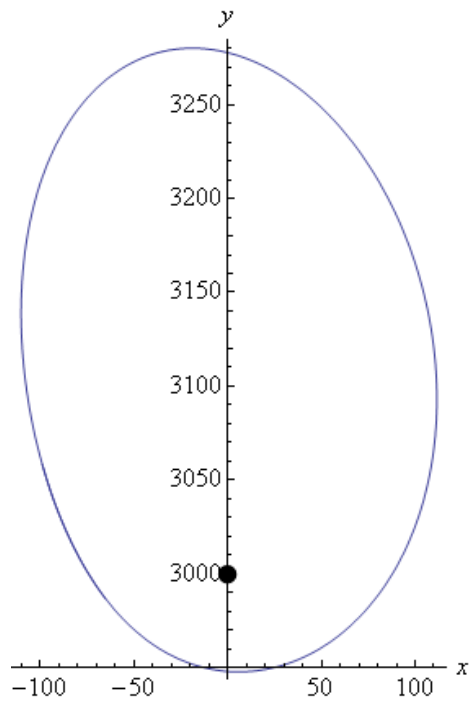


Fig. 8. Vortex orbit with  $Y_0 = 3000$  nm and  $I_{CPP} = 8$  mA. The scales on the axes are in units of nm and the circle indicates the nanocontact position.

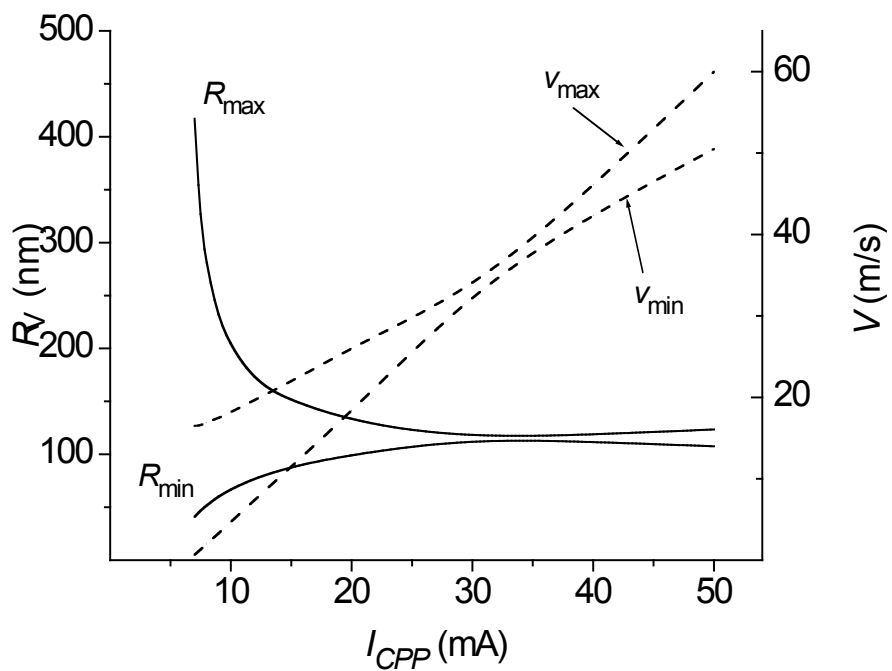


Fig. 9. Solid curves,  $R_{min}$  and  $R_{max}$ . Dashed curves, maximum and minimum velocities at closest and furthest distances from the nanocontact, respectively.